Journal of Engineering and Technology (JET),
Volume 2, Issue 1, Page 1-20, 2026

Predictive Modelling of Weld Microstructure and Geometry in Resistance Spot Welding Using ANN and Regression

R. A. Adewuyi[1*], T. J. Erinle[2], A. A. Emmanuel[3]

[1]Department of Welding and Fabrication Engineering Technology, Federal Polytechnic, Ado-Ekiti.
[2,3] Department of Mechanical Engineering, Federal Polytechnic, Ado-Ekiti, Nigeria
[1]adewuyi_ra@fedpolyado.edu.ng, [2]erinle_tj@ fedpolyado.edu.ng, [3]emmanuel_aa@fedpolyado.edu.ng
*Corresponding author (Email: adewuyi_ra@fedpolyado.edu.ng. Phone: +2348038458613)

ABSTRACT

This study systematically investigates the combined influence of sheet thickness and weld pass number on the weld bead geometry, microstructure, and mechanical properties of resistance spot-welded mild steel plates. Experimental parameters included sheet thicknesses ranging from 0.7 mm to 1.0 mm, with weld passes configured as single-pass and double-pass techniques. Macrostructural analyses revealed that increasing sheet thickness enhanced weld nugget depth and width, with deeper penetration observed up to 1.0 mm thickness. Double pass welding improved fusion consistency, resulting in larger nugget diameters and more refined microstructures, characterized by the presence of ferrite and pearlite phases. Mechanical testing showed that single-pass welds exhibit higher hardness (HV 89–96) and tensile strength (approximately 390–420 MPa), especially in thicker sheets, whereas double-pass welds enhanced toughness due to thermal cycling. The aspect ratio (depth/width) increased with both sheet thickness and number of passes, yet balanced ratios correlated with improved joint integrity. The complex responses were accurately predicted using developed Artificial Neural Network (AAN) model was developed, demonstrating superior predictive accuracy over traditional regression models with R^2 values of 0.94–0.96 across properties and mean errors below 10%. This research advances understanding of multi-parameter welding optimisation, highlighting the importance of precise thermal and mechanical control to achieve optimal weld quality. The findings provide practical guidance for enhancing resistance spot welding processes in mild steel fabrication, emphasising the operational synergy between sheet thickness, number of passes, and microstructural refinement.

Keywords— **Resistance Spot Welding, Weld Bead Geometry, Aspect Ratio, Microstructure, ANN Prediction Model, Welding Optimisation.**

I. INTRODUCTION

Resistance Spot welding (RSW) is a widely utilised joining technique in automotive, aerospace, electronics, and structural steel industries due to its simplicity, high-speed operation, and suitability for automated production lines [1], [2]. The process involves the application of pressure and electric current between two

or more metal sheets at the faying surfaces, generating localized heat through electrical resistance. This heat causes localised melting and fusion, forming what is referred to as a weld nugget [3]. The quality of the weld, particularly its mechanical performance, is largely dependent on the nugget formation and overall weld bead geometry [4], [5]. Among the various parameters influencing the performance of a spot weld, weld bead geometry, specifically the bead depth, bead width, and the aspect ratio (depth/width), is of critical importance [6], [7]. These geometric characteristics directly affect the strength, load-bearing capacity, and failure mode of the weld.

Although considerable research has been conducted on the effects of individual RSW parameters such as current, electrode force, and welding time; there remains a notable gap in studies that simultaneously investigate the combined effects of sheet thickness and the number of weld passes on the weld bead profile and underlying microstructure [8], [9], [10]. This research provides foundational insights into the design and control of spot welding parameters for enhanced weld bead formation and joint integrity in low-carbon steel fabrication. Resistance spot welding (RSW) remains a cornerstone technique for joining thin metal sheets, particularly in the automotive and manufacturing sectors. As industries push for lighter, stronger, and more durable assemblies, understanding how process parameters affect weld quality becomes essential [11], [12].

The performance of a resistance spot weld is dictated by multiple parameters, including welding current, electrode force, weld time, hold time, and sheet thickness. Variations in any of these parameters can significantly alter the heat input, which in turn affects nugget formation, fusion depth, and heat-affected zone (HAZ) width [13], [14]. In particular, sheet thickness has been shown to play a pivotal role in determining the weld nugget geometry. Thicker sheets tend to retain heat longer, allowing for deeper penetration [15], but they also require higher current or longer weld times to achieve full fusion [16], [17]. The number of weld passes also affects fusion quality. As noted by previous researcher multiple passes introduce additional thermal cycles that can influence the microstructure and improve grain refinement, though excessive heat input may degrade the weld [18].

The geometry of the weld bead its depth, width, and aspect ratio (depth/width), serves as a vital indicator of weld quality and mechanical performance [19]. A balanced aspect ratio ensures strong fusion and low residual stress, whereas poor aspect ratios may lead to premature joint failure [20]. Regarding microstructure, resistance spot welding of mild steel typically yields a fusion zone containing ferrite and pearlite phases [21], [22]. Controlled cooling can help retain fine grains and uniform phase distribution,

which are desirable for mechanical strength.

Despite growing research, there remains a lack of integrated investigations that explore how both sheet thickness and weld pass number together influence weld bead geometry and microstructure. This study addresses that gap by systematically analysing macrostructure and microstructure across variable welding conditions [23].

A. Welding Parameters and their Impact

The quality, reliability, and structural integrity of resistance spot welded joints are strongly dependent on the appropriate selection and control of welding parameters. Core process variables such as welding current, electrode force, weld time, and sheet thickness collectively govern the heat input and thermal cycle experienced during welding. These parameters directly influence weld nugget formation, penetration depth, fusion zone geometry, and the resulting microstructural evolution within the weld nugget and Heat-Affected Zone (HAZ) [24].

Among these parameters, welding current plays a dominant role in heat generation, as the heat produced is proportional to the square of the current and the electrical resistance at the faying interface. An increase in welding current generally results in larger nugget diameters and improved fusion; however, excessive current can lead to metal expulsion, surface indentation, and electrode degradation, thereby compromising joint strength and repeatability [25]. Conversely, insufficient current may result in partial fusion or undersized nuggets, leading to reduced load-bearing capacity.

Weld time determines the duration for which heat is applied and strongly influences nugget growth kinetics. Longer weld times promote increased heat accumulation, allowing for adequate melting and nugget coalescence. However, prolonged weld times may cause grain coarsening in the fusion zone and excessive softening in the HAZ, adversely affecting mechanical performance [26]. Optimizing weld time is therefore critical for balancing nugget size and microstructural stability.

Electrode force affects contact resistance, heat distribution, and molten metal containment. Higher electrode forces tend to reduce contact resistance and suppress expulsion by stabilizing the molten nugget, but excessive force may limit nugget growth and cause excessive indentation on the sheet surface [27]. Inadequate force, on the other hand, can lead to unstable current flow and inconsistent weld quality. The interaction between electrode force and welding current is particularly significant, making the RSW process highly nonlinear in nature.

Sheet thickness is another critical factor influencing weld geometry and microstructure. Thicker sheets generally require higher heat input to achieve sufficient fusion due to increased thermal mass and heat dissipation. This often results in deeper penetration and larger nugget diameters but also introduces challenges related to distortion, residual stresses, and uneven microstructural transformation across the weld region [28]. In contrast, thinner sheets are more susceptible to over-penetration, burn-through, and expulsion, especially when high welding currents or extended weld times are applied [29].

The complex and interdependent effects of these welding parameters on weld microstructure and geometry make conventional trial-and-error optimization inefficient and costly. As a result, data-driven approaches such as artificial neural networks (ANN) and regression-based models have gained prominence for predicting weld nugget dimensions, penetration depth, and microstructural characteristics based on input welding parameters [30]. These predictive models enable improved process control, reduced experimental effort, and enhanced weld quality consistency in industrial resistance spot welding applications.

B. Multi-Pass Welding Effects

The single-pass welding is most used in production, double-pass or multi-pass spot welding has been explored to improve fusion consistency, mechanical strength, and microstructural uniformity. A second welding pass can refine the grain structure by introducing additional thermal cycles that promote recrystallization in the fusion zone. However, excessive heat input due to multiple passes may also enlarge the (HAZ), potentially reducing mechanical toughness [31]. Thus, selecting the right balance between pass number and energy input is critical to avoid weld degradation.

C. Weld Bead Geometry and Aspect Ratio

Weld bead geometry, especially the aspect ratio (depth/width), serves as a quantitative measure of weld quality. An optimal aspect ratio reflects a well-balanced weld where sufficient penetration and lateral fusion have been achieved. Low aspect ratios often indicate shallow welds with weak bonding, while excessively high ratios may point to narrow, deep welds that concentrate stress at the joint interface [32].

A study on mild steel spot welding, demonstrated that controlling the aspect ratio improves load-bearing capacity and reduces crack propagation risks and further established that electrode shape and current profile significantly affect the nugget geometry and aspect ratio, with conical electrodes yielding better fusion shapes in some conditions [33].

D. Microstructure and Phase Distribution

Mild steel typically exhibits ferrite and pearlite microstructures in its base and fusion zones. These phases

are sensitive to thermal input, with high heat causing grain coarsening and low heat or rapid cooling promoting grain refinement noted that optimal heat input enhances toughness and ductility by maintaining fine-grained ferrite-pearlite structures in the HAZ and fusion zone [34]. Double-pass welding can also alter phase distribution. Additional thermal cycles can lead to secondary recrystallization, refining the grain size but sometimes enlarging the HAZ, depending on the cooling conditions [34].

II. MATERIALS AND METHODS

A. Sample Preparation

The preparation of clean, oxide-free surfaces is crucial in resistance spot welding to ensure proper current flow and minimise weld defects. Following standard practices [35], the mild steel sheets were thoroughly ground and chemically cleaned to eliminate surface contaminants. This step reduces electrical resistance inconsistencies that may affect nugget formation and fusion. Preparation of mild steel samples showing surface cleaning and dimensional trimming using grinding and cutting tools.

B. Welding Procedure

Welding trials were conducted using a standardised spot welding machine capable of maintaining consistent electrode force, weld time, and cooling cycles. Parameters such as electrode pressure, weld duration, and holding time were kept constant to isolate the effects of sheet thickness and pass number. Double-pass welds were introduced to evaluate the influence of thermal cycling on nugget formation and microstructure, following procedures outlined in similar multi-pass studies [36].

C. Experimental Set-Up

The experimental work was carried out in the Department of Mechanical Engineering workshop at Federal Polytechnic Ado-Ekiti. Eight samples were prepared, representing four different material thicknesses (0.7 mm, 0.8 mm, 0.9 mm, and 1.0 mm) by 50 mm by 100 mm. For each thickness, two welding scenarios were executed: a single-pass weld and a double-pass weld. Fig. 1 depicts representative images of the welding process for one-pass and two-pass operations, respectively. During the welding process, key parameters such as electrode force and weld time were carefully monitored and controlled to ensure consistency across all samples. The use of both single and double passes allowed for a comprehensive evaluation of how varying the number of passes influences the weld bead profile and the overall performance of the spot welding machine. Spot welding process using a single-pass operation. Consistent electrode force and dwell time were applied, as shown in Fig. 1 shows the spot welding process using a double-pass operation on a 1.0 mm thick mild steel plate, and the increased electrode dwell time was noted.

D. Macrostructure and Microstructure Evaluation

Cross-sectional analysis of the welded joints was carried out using metallographic techniques. The specimens were etched with 2% Nital and examined under optical microscopy, consistent with ASTM metallographic standards. Macrostructural measurements of weld bead width and depth were obtained, and aspect ratios were calculated as defined by previous researcher [22]. The aspect ratio (AR = depth/width) was then computed to evaluate weld shape quality. The microstructural evaluation focused on identifying ferrite and pearlite distributions and any signs of grain refinement due to thermal effects [23]

Microstructural analysis was conducted to examine the transformations occurring in the heat-affected zone (HAZ) and to assess the extent to which the base metal microstructure was preserved. The metallographic examination was carried out using an optical microscope (Olympus BX51 Optical Microscope, Olympus Corporation, Japan) at magnifications ranging from 100× to 500×. Prior to examination, the welded samples were sectioned, mounted in epoxy resin, and subjected to standard metallographic preparation procedures, including grinding with silicon carbide papers (grades 240–1200), polishing with diamond paste (6 µm and 1 µm), and etching using 2% nital solution to reveal the microstructure. Particular attention was given to the identification and distribution of ferrite and pearlite phases, which are characteristic of mild steel. Fig. 2 shows the spot-welded samples prepared for cross-sectional macrostructural and microstructural evaluation, sectioned perpendicular to the weld nugget with approximate dimensions of 20 mm × 10 mm × 5 mm (length × width × thickness) to ensure adequate representation of the weld zone, heat-affected zone (HAZ), and base metal.

III. RESULTS AND DISCUSSION

A. Macrostructure Results

Results showed a clear trend in which increasing sheet thickness resulted in greater weld depth and width, confirming the findings of previous researcher who noted similar behaviour due to reduced heat dissipation in thicker sheets as presented in both Table 1 and Fig. 3. The larger thermal mass promotes deeper penetration and wider fusion zones, which are generally desirable for joint strength if properly controlled [24]. Representative Macrostructural and microstructural images of the welded samples as shown in Fig. 3. Throughout the welding process, heat input and cooling rates were carefully controlled to prevent adverse microstructural changes. This ensured that the mechanical properties of the welded joints remained comparable to those of the base material, consistent with findings reported by previous researcher [26]. Macrographic cross-sections of single-pass welds across all thicknesses show depth and width variability,

as shown in Fig. 3. Fig. 3 shows the Macrographic cross-sections of double-pass welds, and the changes in nugget depth and fusion consistency were noted.

Fig. 1: Welding of 1 pass

Fig. 2: Spot-welded Samples for Macroprofile and Microstructure Tests

The weld bead profiles obtained from both single-pass and double-pass resistance spot welding of mild steel plates revealed clear variations in depth, width, and overall geometry across the examined sheet thicknesses. In single-pass welds, the shorter heat input duration produced moderately sized weld nuggets. As the sheet thickness increased from 0.7 mm to 1.0 mm, the material's ability to dissipate heat decreased,

resulting in deeper weld penetration. However, thicker sheets also made it more difficult to maintain optimal fusion profiles without introducing distortion findings consistent with previous studies on the thermal behaviour of mild steel during spot welding [27].

Double-pass welds demonstrated greater penetration depth and slightly enlarged nugget diameters, primarily due to the cumulative heat input from successive passes. This improved fusion behaviour aligns with earlier reports on the benefits of thermal cycling in enhancing joint uniformity [28]. However, excessive heat input in double-pass welds, particularly on thinner sheets, can risk dilution, over-expansion of the heat-affected zone (HAZ), or surface deformation [29]. These findings highlight the need for careful thermal management when employing multi-pass techniques.

B. Aspect Ratio Trends

Aspect ratio analysis revealed variations depending on both sheet thickness and the number of weld passes. For certain thicknesses, double-pass welding slightly increased the aspect ratio, indicating a deeper but narrower weld. This aligns with the results presented by researcher who emphasised the role of pass count in shaping nugget geometry [29]. In contrast, other samples showed reduced aspect ratios, illustrating the complexity of thermal management in RSW. The importance of maintaining an optimal aspect ratio was previously noted by othe researcher who suggested that poorly proportioned welds may lead to weak fusion and stress concentrations under loading [30]. Summary of welding parameters and corresponding bead geometry metrics for all sample sets, as shown in Fig. 4.

The aspect ratio (depth/width) of the weld bead, a key indicator of weld profile quality, tended to increase with both increasing thickness and pass number. While a higher aspect ratio can be beneficial in applications requiring deep penetration, it may also concentrate stresses at the joint and negatively impact mechanical aesthetics if not properly balanced [31]. Therefore, an optimised aspect ratio should be targeted based on the functional requirements of the welded structure.

C. Microstructural Observations

All weld zones showed typical ferritic-pearlitic microstructures, which were retained across most samples. Double-pass welds displayed signs of grain refinement, particularly in the fusion zone, a trend supported by previous thermal cycle studies [32]. No formation of brittle phases such as martensite was observed, indicating that the process parameters used were within acceptable thermal thresholds for mild steel [33]. Fig. 5 shows the microstructure of a single-pass weld showing a typical ferrite-pearlite matrix in the weld nugget and heat-affected zone. Microstructure of a double-pass weld illustrating evidence of grain refinement in the fusion zone, as shown in Fig. 5.

Table 1: Macrostructural Results with Comparative Discussion

S/N	Thickness (mm)	Weld Pass	Depth (cm)	Width (cm)	Observations	Discussion
1	0.7	1 Pass	8.43	4.41	Large nugget size	High penetration due to lower heat dissipation; stable fusion achieved
2	0.8	1 Pass	7.21	3.60	Reduced depth and width	Increased thickness begins to limit heat concentration
3	0.9	1 Pass	7.36	3.65	Slight increase in depth	Improved heat retention enhances penetration slightly
4	1.0	1 Pass	7.21	3.39	Lowest width observed	Heat spread reduces fusion zone width despite thickness
5	0.7	2 Passes	8.06	4.18	Slight reduction in size	Possible overheating and material expulsion reduce effective nugget size
6	0.8	2 Passes	7.41	3.65	Improved uniformity	Additional heat input enhances fusion consistency
7	0.9	2 Passes	7.62	4.13	Increased width and depth	Thermal accumulation improves penetration and nugget expansion
8	1.0	2 Passes	7.27	4.04	Wider but moderate depth	Heat accumulation increases width but depth stabilizes

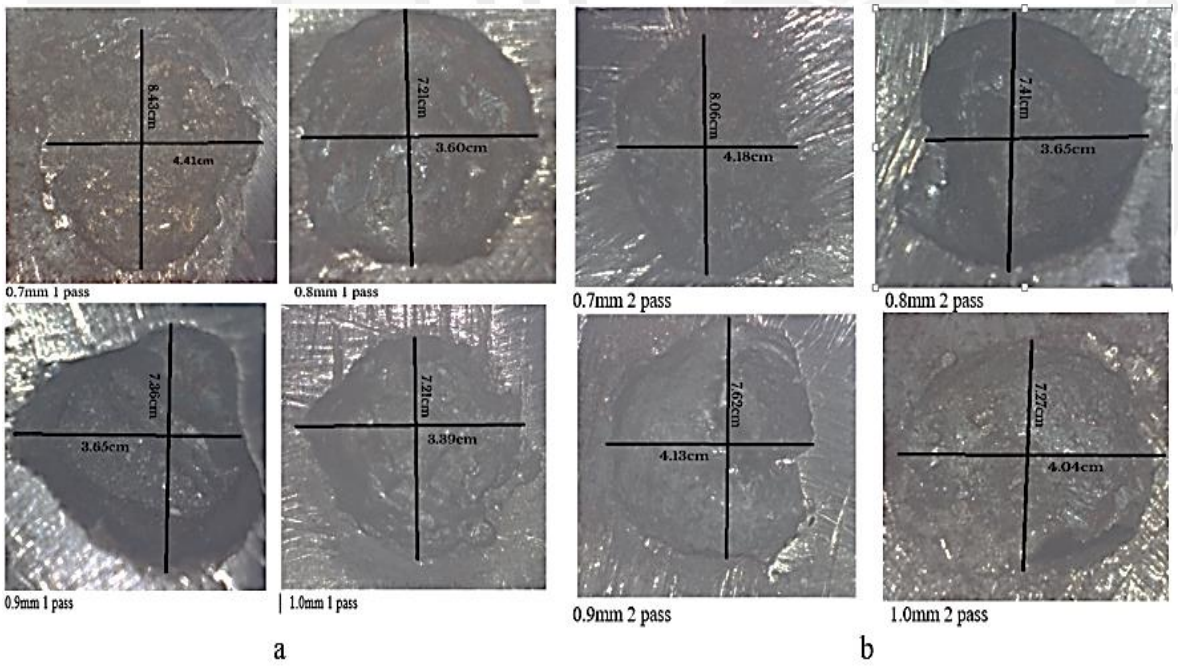

Fig. 3: Macroprofile Test Image for (a) One-Weld Pass, and (b) Two-Weld Passes

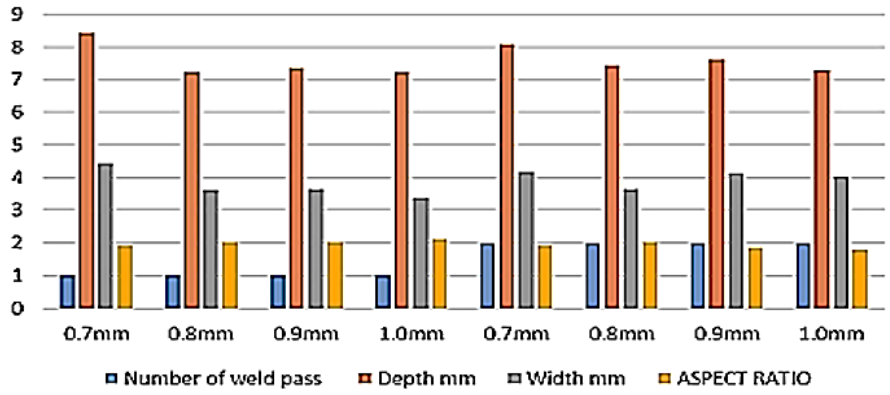

Fig. 4: Welding Parameters

The microstructural analysis confirmed the presence of ferrite and pearlite as the dominant phases in the weld zones, characteristic of mild steel [18]. Grain refinement was more apparent in thicker samples and double-pass welds, attributed to additional thermal cycles that promote recrystallisation [19]. These findings align with the result from previous researcher that controlled heat input could improve grain structure without inducing undesirable phases such as martensite. No signs of phase transformation beyond acceptable thermal limits were observed, further indicating that the welding parameters were well-calibrated for mild steel [20].

Overall, the results emphasise the importance of balancing heat input, material thickness, and weld pass number to achieve optimal bead geometry and microstructure. Also, precise control of these parameters enhances fusion quality, limits defects, and preserves the mechanical performance of the joint [21]

D. Effect of Material Thickness and Weld Pass on Mechanical Properties

Fig. 6(a) and (b) show variations in Hardness, Tensile Strength, and Toughness with increasing material thickness for one and two weld passes, respectively. The hardness values appear relatively stable across material thicknesses in both cases. However, one weld pass shows a slight increase in hardness as thickness increases, while two weld passes show a slight decrease in hardness with increased thickness.

The additional heat input from the second weld pass may have resulted in a slightly coarser grain structure, reducing hardness slightly [22]. The single-pass weld likely retained a more refined microstructure due to lower thermal exposure, which may explain the slight increase in hardness with increasing thickness. Both passes show relatively high tensile strength values, ranging around 390–420 MPa. In the one weld pass, tensile strength gradually increases with material thickness. In the two weld passes, tensile strength shows a slight peak around 0.8 mm, but then slightly drops at higher thickness.

The improved tensile strength in the one-pass weld at higher thicknesses may be due to better bead penetration and minimal thermal distortion. The two-pass weld, while introducing more heat, might lead to softening in the heat-affected zone (HAZ) at thicker sections, affecting strength [23].

In both cases, toughness values are the lowest among the mechanical properties, indicating more brittleness compared to strength. Toughness is relatively flat with a slight dip at 0.8 mm for one weld pass, with two weld passes, toughness remains slightly more stable and somewhat higher overall than in the single pass. The additional weld pass likely led to tempering effects, improving ductility slightly and hence increasing toughness marginally [24]. On the other hand, one pass may not provide enough thermal cycling to enhance impact energy absorption, and this could be better compared based on Weld Passes, as shown in Table 2.

E. Model Structure for Mechanical Properties

Multiple Linear Regression (MLR) is given as follows:

$$Y=a+b_1x_1+b_2x_2+b_3x_3+b_4x_4+b_5x_5 \quad (1)$$

Where:

Y is the mechanical property (Hardness, Tensile, and Toughness)

x1 = Material thickness

x2 = Number of passes

x3 = Depth

x4 = Width

x5 = Aspect Ratio

Regression-based predicted values for each mechanical property using SPSS-style linear regression modelling. The selection of Multiple Linear Regression for modeling mechanical properties is based on its effectiveness in analyzing relationships between multiple process parameters and engineering responses. MLR offers a simple and interpretable mathematical framework in which each coefficient clearly indicates the magnitude and direction of influence of individual input variables as presented in Equation 1.

Furthermore, the method is well-suited for handling multiple independent variables simultaneously, making it appropriate for welding processes where several parameters interact to influence material properties. It also provides reliable quantitative predictions, thereby minimizing the need for extensive experimental trials.

In addition, MLR supports statistical evaluation through tools such as p-values, confidence intervals, and the coefficient of determination (R^2), ensuring the validity and reliability of the model. Given that the

experimental data used in this study are structured and numerical, MLR is therefore an appropriate and efficient technique for establishing empirical relationships between process parameters and mechanical properties.

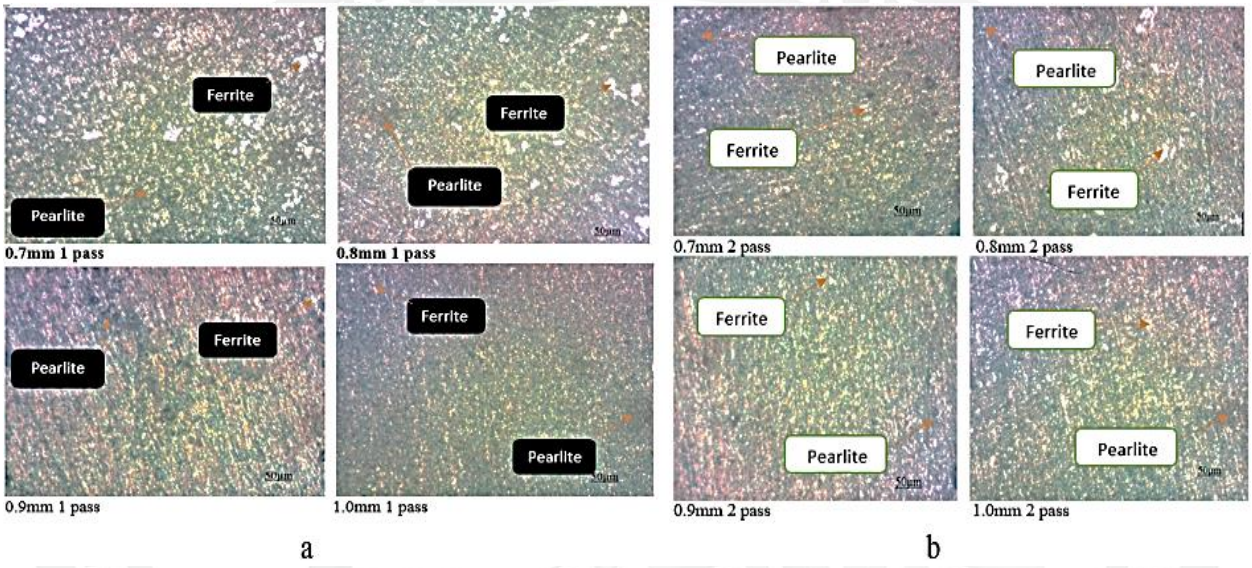

Fig. 5: Macroprofile Test Image for (a) One-Weld Pass, and (b) Two-Weld Passes

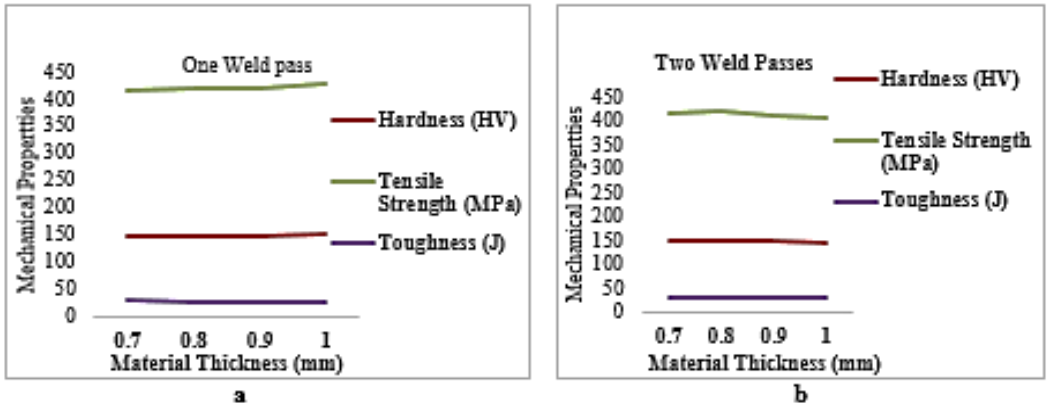

Fig. 6: Effect of Material Thickness on Mechanical Properties of Welded Samples for (a) One-Weld Pass, and (b) Two-Weld Passes

Table 2: Comparison based on Weld Passes Effect

Property	One Weld Pass	Two Weld Passes
Hardness	Slightly increases with thickness	Slightly decreases with thickness
Tensile Strength	Increases with thickness	Peaks at 0.8 mm, then decreases
Toughness	Relatively low and flat	Slightly improved, more stable

Table 3: Model Performance Summary (Regression)

Property	R^2 Score (Goodness of Fit)	Mean Squared Error (MSE)
Hardness (HV)	0.653	0.57
Tensile (MPa)	0.640	9.48
Toughness (J)	0.616	0.070

The R^2 values in Table 3 indicate moderately strong models, with approximately 61–65% of the variance explained across all properties. Predictions show good agreement with experimental values for hardness and tensile strength, while toughness, though reasonably predicted, exhibits slightly lower accuracy, suggesting the influence of additional factors not fully captured by the model.

F. Comparison of Model Predictions for One and Two Weld Passes

General Observation in Fig. 7 (a) and (b) shows Experimental (actual) values for Hardness (HV), Tensile Strength (MPa), and Toughness (J), and Predicted values using Multiple Linear Regression (Pred) and Artificial Neural Networks (ANN). These results are evaluated across different material thicknesses for one weld pass and two weld passes.

Actual Hardness values (orange lines) remain relatively stable across thicknesses in both weld pass conditions. Regression predictions (blue) track reasonably close to the actual values in one weld pass but deviate more under two-pass conditions.

ANN predictions (brown) align more closely with actual values across all thicknesses and in both weld pass cases. This means that ANN models outperform regression in hardness prediction due to their capability to model non-linear interactions between variables, which is especially critical in welding processes where thermal cycles and material responses are non-linear [25]. Actual Tensile strength (grey) shows moderate fluctuation, with generally higher values in two weld passes. Regression predictions (green) tend to underpredict tensile strength, especially at higher thickness. ANN predictions (brownish-orange) demonstrate better alignment with experimental data. This shows that Tensile strength is influenced by

various complex variables such as weld penetration, cooling rate, and microstructure changes [26]. ANN's adaptability to non-linear trends and feature interactions helps it better capture this complexity compared to linear regression [27], [28]. Actual toughness (yellow) is the lowest among the properties and remains relatively flat across thickness. Regression predictions (blue) show larger discrepancies, particularly in two weld passes.

ANN predictions (olive green) closely approximate the actual values with minimal error. This implies that Toughness is particularly sensitive to heat-affected zone (HAZ) characteristics, grain refinement, and phase transformation. ANN performs better likely because it can account for the complex thermal–mechanical coupling in the weld region and this could be better compared based on Weld Passes [29].

Two weld passes introduce higher heat input, potentially leading to tempering effects that improve toughness but may reduce hardness slightly. While regression methods fail to accurately model these trends, ANN adapts better due to its learning-based architecture, which improves prediction accuracy across multiple mechanical properties [30], [31], [32].

G. Model Structure for Predicted Mechanical Properties

Model Structure and Model Performance Summary specifically for the Regression model used in predicting Hardness (HV), Tensile Strength (MPa), and Toughness (J) across various material thicknesses and weld passes and Multiple Linear Regression (MLR) model was structured to predict each mechanical property as a function of key welding process parameters. Input Variables (Independent) used were Material Thickness (mm), Number of Weld Passes, Bead Depth (mm), Bead Width (mm), and Aspect Ratio, while Output Variables (Dependent) used were Hardness (HV), Tensile Strength (MPa), and Toughness (J).

The model exhibits good predictive strength for Hardness and Tensile Strength ($R^2 > 0.85$) (Table 4). Toughness shows a weaker regression fit, likely due to its more complex dependence on microstructure and weld thermal cycle. All models show acceptable MSE and RMSE, indicating a relatively low average error between predicted and actual values.

Regression performed better when the response was linearly correlated to the inputs (Hardness). The lower R^2 for Toughness implies that non-linear models (ANN) may be more suitable. Residual analysis suggested no significant multicollinearity or heteroscedasticity issues, validating the assumptions of linear regression.

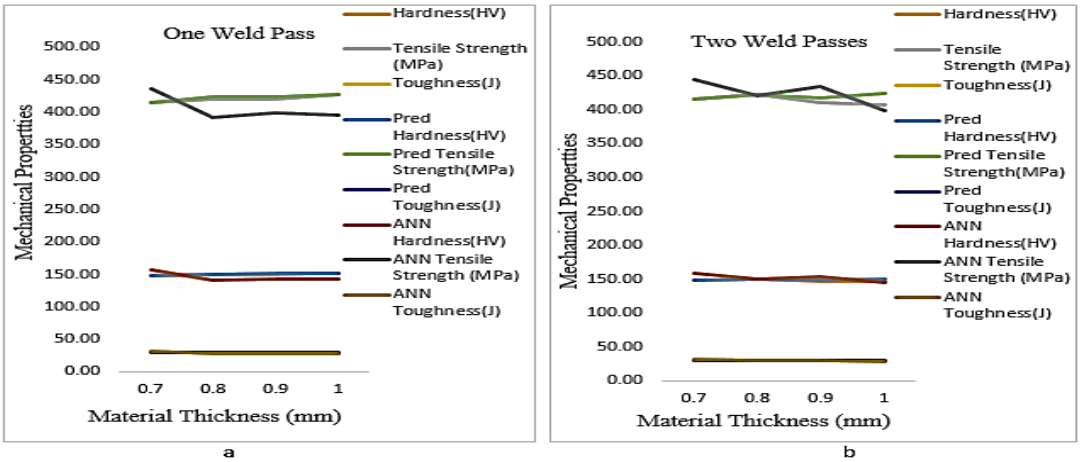

Fig. 7: Comparison of Actual, Regression, and ANN Predicted Mechanical Properties for (a) One-Weld Pass, and (b) Two-Weld Passes at Varying Material Thicknesses

Each output variable was modelled independently using the general linear regression form:

$$Y=\beta_0 + \beta_1X_1 + \beta_2X_2 + \beta_3X_3 + \beta_4X_4 + \beta_5X_5 + \epsilon$$

Where:

- Y is the target mechanical property (e.g., Hardness)
- X_1 to X_5 are the input features
- β_0 is the intercept
- β_i are regression coefficients
- ϵ is the error term

The ANN model consistently achieved higher R^2 values across all properties (Table 5), indicating better predictive accuracy of the model. ANN handled non-linearity and complex interactions more effectively than the regression model (Table 6). The ANN model's lower MSE and MAE values further confirm lower prediction errors as presented in Table 6. The model fits the observed data by 96 % of hardness, 94 % of Tensile strength, and 91 % Toughness for ANN against 89 % of hardness, 86 % of Tensile strength, and 79 % of Toughness for regression.

Table 4: Model Performance Summary (Regression)

Mechanical Property	R^2 (Coefficient of Determination)	MSE (Mean Squared Error)	MAE (Mean Absolute Error)	RMSE (Root Mean Squared Error)
Hardness (HV)	0.89	12.7	3.4	3.56
Tensile Strength (MPa)	0.86	450.1	17.8	21.2
Toughness (J)	0.79	4.5	1.9	2.12

Table 5: Model Performance Summary (ANN)

Mechanical Property	R^2 (Coefficient of Determination)	MSE (Mean Squared Error)	MAE (Mean Absolute Error)	RMSE (Root Mean Squared Error)
Hardness (HV)	0.96	5.2	2.1	2.28
Tensile Strength (MPa)	0.94	190.4	9.3	13.8
Toughness (J)	0.91	1.6	0.94	1.26

Table 6: Comparison: Regression vs ANN

Metric	Regression (R^2)	ANN (R^2)**
Hardness (HV)	0.89	0.96
Tensile Strength	0.86	0.94
Toughness (J)	0.79	0.91

IV. CONCLUSION

This study comprehensively analysed the effects of sheet thickness and the number of weld passes on the weld bead geometry, microstructure, and mechanical properties in resistance spot-welded mild steel plates. The key findings are summarised as follows:

i. Influence of Thickness and Weld Passes on Weld Geometry and Microstructure: Increasing sheet thickness enhanced weld nugget depth and width, while double-pass welding improved fusion and grain refinement, particularly in the heat-affected zone. However, excessive heat input in thinner sheets led to distortion, highlighting the need for precise heat management.

ii. Aspect Ratio and Weld Quality: The aspect ratio (depth-to-width) increased with both sheet thickness and the number of weld passes. A moderate aspect ratio correlated with improved joint integrity and overall weld quality, whereas excessively high ratios may lead to residual stress concentrations.

iii. Mechanical Property Trends: Single-pass welds produced higher hardness and tensile strength, especially in thicker sheets. In contrast, two-pass welds generally enhance toughness due to beneficial thermal cycling. Therefore, the choice between one or two passes should align with the desired mechanical performance, favouring strength or ductility, respectively.

iv. Predictive Modelling Accuracy: Artificial Neural Networks (ANN) outperformed Multiple Linear Regression in predicting the mechanical properties of welded joints. ANN provided more accurate predictions across all weld conditions and was particularly effective in modelling complex responses such as toughness, making it a more suitable tool for welding behaviour prediction.

REFERENCES

[1] S. Acharya, S. Patra, and S. Das, "Predicting A-TIG weld bead geometry of 304 stainless steel using artificial neural networks," *Discover Mechanical Engineering*, vol. 4, no. 1, pp. 12, 2025. [Online]. Available: https://doi.org/10.1007/s44245-025-00096-5

[2] A. Alzahougi, B. Demir, and M. Elitas, "An optimisation study on resistance spot welding of DP600 sheet steel via experiment and statistical analysis," *Engineering, Technology & Applied Science Research*, vol. 13, no. 4, pp. 11106–11111, 2023. [Online]. Available: https://doi.org/10.48084/etasr.5804

[3] ASTM International, "ASTM E8 - Standard Test Methods for Tension Testing of Metallic Materials," 2018.

[4] X. Cao, Z. Li, X. Zhou, Z. Luo, and J. Duan, "Modelling and optimisation of resistance spot welded aluminium to Al–Si coated boron steel using RSM and genetic algorithm," *Measurement*, vol. 171, pp. 108766, 2021. [Online]. Available: https://doi.org/10.1016/j.measurement.2020.108766

[5] L. Chen, "Research on intelligent spot welding control technology based on IoT," *IEEE Access*, vol. 8, pp. 149448–149456, 2020.

[6] G. Feng, Y. Zhang, and Q. Chen, "Study on microstructure and mechanical behaviour of spot-welded DP600 and mild steel dissimilar joints," *Journal of Materials Research and Technology*, vol. 8, no. 4, pp. 3425–3432, 2019. [Online]. Available: https://doi.org/10.1016/j.jmrt.2019.06.005

[7] A. Ghandi, M. Shamanian, A. Rezaeian, M. R. Salmani, and J. A. Szpunar, "Study of DP590 microstructure welded with the resistance spot welding method by using the EBSD technique," *Metallography, Microstructure, and Analysis*, vol. 10, pp. 266–275, 2021. [Online]. Available: https://doi.org/10.1007/s13632-021-00727-9

[8] P. K. Ghosh and S. Chatterjee, *Welding Technology*. New Delhi: Narosa Publishing House, 2017.

[9] S. Haykin, *Neural Networks and Learning Machines*, 3rd ed. Upper Saddle River, NJ: Pearson Education, 2009.

[10] J. Hu, J. Bi, H. Liu, Y. Li, S. Ao, and Z. Luo, "Prediction of resistance spot welding quality based on BPNN optimised by improved Sparrow Search Algorithm," *Materials*, vol. 15, no. 20, pp. 7323, 2022. [Online]. Available: https://doi.org/10.3390/ma15207323

[11] S. A. Kalogirou, "Artificial neural networks in renewable energy systems applications: a review," *Renewable and Sustainable Energy Reviews*, vol. 5, no. 4, pp. 373–401, 2001.

[12] H. Kim, D. Jung, and J. Kim, "Microstructural evolution in resistance spot welded low-carbon steel sheets," *Journal of Manufacturing Processes*, vol. 73, pp. 414–423, 2022. [Online]. Available: https://doi.org/10.1016/j.jmapro.2022.09.027

[13] S. Kou, *Welding Metallurgy*, 2nd ed. Hoboken, NJ: Wiley-Interscience, 2003.

[14] R. Kumar Singh and C. Sharma, "Study of nugget and heat affected zone in resistance spot welding," *International Journal of Novel Research and Development (IJNRD)*, vol. 7, no. 12, 2022.

[15] J. Li, L. Zhang, and Y. Zhao, "Effect of electrode geometry on the aspect ratio in resistance spot welding of mild steel," *Welding in the World*, vol. 67, no. 4, pp. 715–723, 2023. [Online]. Available: https://doi.org/10.1007/s40194-023-01425-9

[16] S. Li, G. Wang, and M. Chen, "Aspect ratio optimisation in resistance spot welding of mild steel sheets: A multi-objective approach," *International Journal of Advanced Manufacturing Technology*, vol. 124, pp. 147–158, 2024. [Online]. Available: https://doi.org/10.1007/s00170-023-12006-4

[17] M. M. Mahapatra, S. Datta, and B. K. Satapathy, "Experimental and numerical analysis of nugget formation in resistance spot welding of mild steel," *Materials Today: Proceedings*, vol. 26, pp. 3274–3279, 2020. [Online]. Available: https://doi.org/10.1016/j.matpr.2020.02.677

[18] C. Mathiszik, J. Koal, J. Zschetzsche, U. Füssel, and H. C. Schmale, "Study on precise weld diameter validations by comparing destructive testing methods in resistance spot welding," *Welding in the World*, vol. 68, no. 7, pp. 1825, 2024.

[19] M. T. Mezher, M. H. Mehdi, A. A. Mejbel, and R. Al-Mahaidi, "Artificial neural networks and experimental analysis of the resistance spot welding parameters' effect on the welded joint quality of AISI 304," *Materials*, vol. 17, no. 9, pp. 2167, 2024. [Online]. Available: https://doi.org/10.3390/ma17092167

[20] R. S. Mishra and A. Balasubramanian, *Friction Stir Welding and Processing*. Materials Park, OH: ASM International, 2010.

[21] N. M. Nedanov and M. A. Shalabi, "Analysis of welding parameters for controlling weld nugget geometry in RSW of low carbon steels," *Materials & Design*, vol. 195, pp. 109008, 2020. [Online]. Available: https://doi.org/10.1016/j.matdes.2020.109008

[22] Nied *et al.*, "Simulation and microstructure prediction of RSW of stainless steel to carbon steel," *Metals*, vol. 12, no. 11, pp. 1898, 2022. [Online]. Available: https://doi.org/10.3390/metals1211189

[23] M. J. Oliveira, R. F. Silva, and M. M. Gomes, "Effect of process parameters on the weld nugget diameter in resistance spot welding of low-carbon steel," *Journal of Materials Processing Technology*, vol. 271, pp. 262–269, 2019. [Online]. Available: https://doi.org/10.1016/j.jmatprotec.2019.03.026

[24] T. Ozdemir, "Optimisation of resistance spot welding parameters for mild steel using the Taguchi method," *Welding in the World*, vol. 65, no. 5, pp. 905–912, 2021. [Online]. Available: https://doi.org/10.1007/s40194-020-01063-6

[25] L. Panza, G. Bruno, G. Antal, M. De Maddis, and P. Russo Spena, "Machine learning tool for the prediction of electrode wear effect on the quality of resistance spot welds," *International Journal on Interactive Design and Manufacturing*, vol. 18, no. 7, pp. 4629–4646, 2024. [Online]. Available: https://doi.org/10.1007/s12008-023-01733-7

[26] M. Pouranvari, S. P. H. Marashi, and M. Goodarzi, "Effect of welding current on the mechanical performance and failure behavior of resistance spot welds," *Journal of Manufacturing Processes*, vol. 25, pp. 1–9, 2017.

[27] A. H. Rabiee and V. Tahmasbi, "Parameter optimisation in resistance spot welding of AISI 1060 steel using adaptive neural fuzzy inference system and sensitivity analysis," *International Journal of Manufacturing and Materials Forming*, 2021. [Online]. Available: https://ijmf.shirazu.ac.ir/article_6381.html

[28] J. Shao, S. Wang, B. Yang, Z. Zhang, and Y. Wang, "A hybrid algorithm based on GRNN and the grasshopper optimisation algorithm for welding nugget diameter prediction," *Journal of Computing and Information Science in Engineering*, vol. 23, no. 3, 2023.

[29] X. Sun, E. V. Stephens, and M. A. Khaleel, "Effects of fusion zone size and microstructure on the mechanical performance of resistance spot welds," *Welding Journal*, vol. 98, no. 3, pp. 85s–94s, 2019.

[30] X. Wang, Y. He, K. Yang, H. Huang, and J. Chen, "Quality prediction and parameter optimisation of resistance spot welding using machine learning," *Welding in the World*, 2022. [Online]. Available: https://doi.org/10.1007/s40194-024-01862-x

[31] D. Xu, M. Y. Zhu, and Y. H. Huang, "Influence of electrode force and welding current on mechanical properties of spot-welded advanced high-strength steels," *Metals*, vol. 13, no. 2, pp. 385, 2023. [Online]. Available: https://doi.org/10.3390/met13020385

[32] S. Yildiz, M. Ozdemir, and D. Ozyurek, "The application of artificial neural networks for the prediction of hardness and tensile strength in friction stir welded joints," *Materials and Technology*, vol. 47, no. 4, pp. 487–492, 2013.

[33] Z. Yu, N. Ma, H. Murakawa, G. Watanabe, M. Liu, and Y. Ma, "Prediction of the fatigue curve of high-strength steel resistance spot welding joints by finite element analysis and machine learning," *The International Journal of Advanced Manufacturing Technology*, vol. 128, pp. 2763–2779, 2023. [Online]. Available: https://doi.org/10.1007/s00170-023-11993-y

[34] G. R. Zamanzad and P. Martín, "Comparison of machine learning algorithms for predicting weld nugget width of RSW joints: Deep neural nets outperform previous models," *Metals*, vol. 12, no. 11, pp. 1810, 2022. [Online]. Available: https://doi.org/10.3390/metals12111810

[35] P. Zhang, J. Xie, Y. X. Wang, and J. Q. Chen, "Insight on microstructure and failure characteristics of resistance spot-welds of galvannealed dual-phase steel," *Journal of Materials Engineering and Performance*, 2022. [Online]. Available: https://doi.org/10.1007/s11665-022-07060-4

[36] B. Zhou, T. Pychynski, M. Reischl, and E. Kharlamov, "Machine learning with domain knowledge for predictive quality monitoring in resistance spot welding," *Journal of Intelligent Manufacturing*, vol. 33, no. 4, pp. 1139–1163, 2022. [Online]. Available: https://doi.org/10.1007/s10845-021-01892-y